4-1-2017

The Arabidopsis kinesin-4, FRA1, requires a high level of processive motility to function correctly

Anindya Ganguly

Logan DeMott

Ram Dixit
Washington University in St Louis, ramdixit@WUSTL.EDU

The *Arabidopsis* kinesin-4, FRA1, requires a high level of processive motility to function correctly

Anindya Ganguly, Logan DeMott* and Ram Dixit‡

ABSTRACT

Processivity is important for kinesins that mediate intracellular transport. Structure–function analyses of N-terminal kinesins (i.e. kinesins comprising their motor domains at the N-terminus) have identified several non-motor regions that affect processivity *in vitro*. However, whether these structural elements affect kinesin processivity and function *in vivo* is not known. Here, we used an *Arabidopsis thaliana* kinesin-4, called Fragile Fiber 1 (FRA1, also known as KIN4A), which is thought to mediate vesicle transport, to test whether mutations that alter processivity *in vitro* lead to similar changes in behavior *in vivo* and whether processivity is important for the function of FRA1. We generated several FRA1 mutants that differed in their 'run lengths' *in vitro* and then transformed them into the *fra1-5* mutant for complementation and *in vivo* motility analyses. Our data show that the behavior of processivity mutants *in vivo* can differ dramatically from *in vitro* properties, underscoring the need to extend structure–function analyses of kinesins *in vivo*. In addition, we found that a high density of processive motility is necessary for the physiological function of FRA1.

KEY WORDS: **Kinesin, Motor protein, Intracellular transport, Single molecule, Live imaging**

INTRODUCTION

Kinesins execute various cellular functions either by powering directional transport of cargo along microtubules or by regulating the dynamics of microtubule ends. Transport kinesins, such as kinesin-1, -2 and -3 family members, mediate long-distance transport of diverse cargo including vesicles, protein complexes and nucleic acids (Hall and Hedgecock, 1991; Kanai et al., 2000; Kondo et al., 1994; Okada et al., 1995; Vale et al., 1985; Verhey et al., 2001). While some microtubule regulatory kinesins, such as kinesin-13 family members, are non-motile, others such as kinesin-4 and kinesin-8 family members are motile but work primarily to regulate the dynamics of microtubule plus-ends (Bringmann et al., 2004; Desai et al., 1999; Gupta et al., 2006; Kurasawa et al., 2004; Varga et al., 2006; Walczak et al., 1996).

Plants contain a large number of kinesins, but little is known about which ones are used for transport and microtubule regulatory functions (Richardson et al., 2006; Zhu and Dixit, 2012). Since kinesin-1, -2 and -3 family members are absent in plants, other classes of kinesins probably perform plus-end-directed transport

Biology Department, Washington University in St. Louis, St. Louis, MO 63130, USA.
*Present address: Department of Plant Sciences, University of California, Davis, CA 95616, USA.

‡Author for correspondence (ramdixit@wustl.edu)

R.D., 0000-0001-7881-2859

functions. Recently, a plant kinesin-4 member, called Fragile Fiber 1 (FRA1, also known as KIN4A), was shown to mediate trafficking of cell wall material along cortical microtubules (Kong et al., 2015; Zhu et al., 2015). Loss of the FRA1 kinesin in a *fra1-5* mutant leads to thinner cell walls, reduced rate of pectin secretion and accumulation of Golgi-associated vesicles, which together indicate that FRA1 likely transports vesicles for secretion. In contrast, both microtubule plus-end dynamics and array organization are unaltered in this mutant (Zhu et al., 2015), demonstrating that, unlike metazoan kinesin-4 proteins, FRA1 does not regulate microtubule plus-end growth.

Transport kinesins have a common structural organization consisting of a catalytic head domain, a flexible neck linker that mediates inter-head communication and amplifies conformational changes needed for motion, a coiled-coil stalk and cargo-binding tail domain. Another shared feature of transport kinesins is their ability to move processively (i.e. take many steps upon binding to a microtubule), which enables efficient long-distance transport by single motors (Howard et al., 1989; Soppina et al., 2014; Yamazaki et al., 1995). Consistent with a transport function, dimeric FRA1 motors have been found to move processively both *in vitro* and *in vivo* (Kong et al., 2015; Zhu and Dixit, 2011; Zhu et al., 2015). To directly investigate the importance of FRA1 processivity for its physiological function, we generated several mutants by modifying different non-motor domains predicted to alter their 'run length' and studied them by using *in vitro* motility assays, as well as genetic complementation and live-imaging in *Arabidopsis thaliana* plants. Our data show that the *in vitro* and *in vivo* motile properties of FRA1 can vary depending on the configuration of the mutant. Furthermore, we found that a high level of processive motility is critical for FRA1 function.

RESULTS AND DISCUSSION
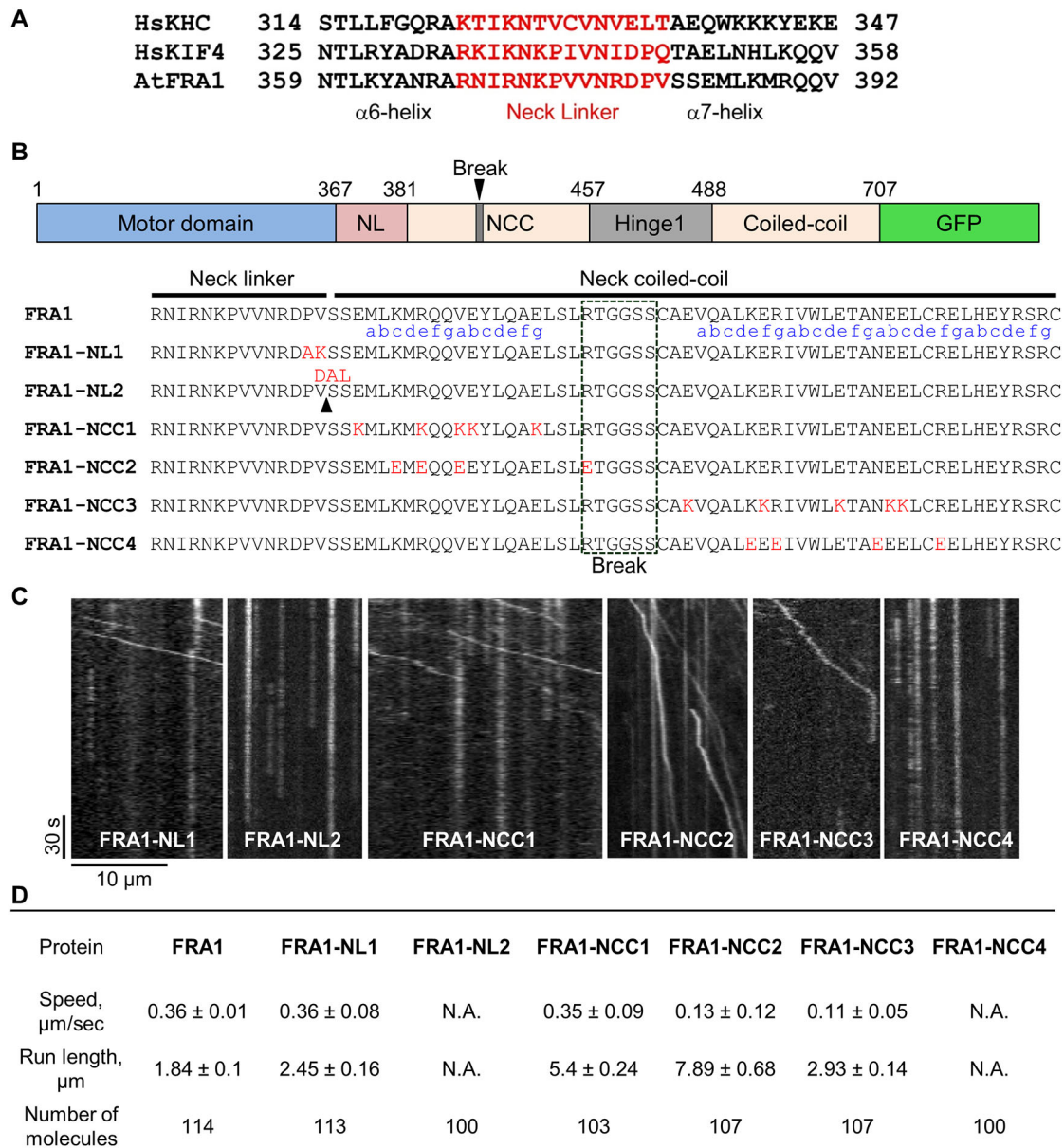### Mutating neck-linker and neck coiled-coil regions alters FRA1 processivity *in vitro*

In vitro experiments have shown that processivity of kinesins can be tuned by altering the length and charge of the neck linker domain and the charge of the neck coiled-coil domain (Shastry and Hancock, 2010, 2011; Thorn et al., 2000). To identify these domains in the FRA1 kinesin, we aligned the amino acid sequences of the motor domains of FRA1 and kinesin-1 to define the start of the neck linker, and used the PCOILs and Multicoil programs to predict the start of the neck coiled-coil. These analyses indicated that the neck linker of FRA1 is 14 amino acids long, similar to that of human kinesin-1 and kinesin-4 (also known as KIF5B and KIF4A, respectively) (Fig. 1A).

To test whether mutations in the neck linker and neck coiled-coil domains affect FRA1 processivity, we conducted single-molecule *in vitro* motility assays with a green fluorescent protein (GFP)-labeled truncated version of FRA1, called FRA1(707)–GFP, which was previously shown to move processively as a dimer *in vitro* (Zhu and Dixit, 2011). We generated two mutants that changed the length and

Fig. 1. *In vitro* motility analysis of FRA1 neck-linker and neck coiled-coil mutants. (A) Sequence alignment of neck linker and flanking α-helices of human kinesin-1 heavy chain (HsKHC), a human kinesin-4 member (HsKIF4) and *Arabidopsis* FRA1 (AtFRA1). The neck linker regions are shown in red. (B) Schematic representation of the structural domains of the first 707 amino acids of the FRA1 kinesin fused with GFP. The amino acid sequences below show the mutations used in this study in red. The predicted heptad repeats in the neck coiled-coil are shown in blue. The arrowhead in FRA1-NL2 indicates the position where the DAL peptide was inserted. NL, neck linker; NCC, neck coiled-coil. (C) Kymographs of the FRA1 mutants from *in vitro* single-molecule motility assays. (D) Motility parameters of wild-type and mutant FRA1 kinesins calculated from the *in vitro* experiments. N.A., not applicable because of lack of directional motility. Values are mean±s.d.

charge of the neck linker domain: FRA1-NL1, in which the PV residues of the neck linker were replaced with AK, and FRA1-NL2 in which a 3-amino-acid DAL peptide was inserted after the PV residues (Fig. 1B). The NL1 mutation was expected to enhance processivity by creating a straighter and more positively charged neck linker, while the NL2 mutation was expected to reduce processivity by overextending the neck linker (Shastry and Hancock, 2010). We found that FRA1-NL1 had ~30% increased processivity and unchanged speed compared to wild-type FRA1, while FRA1-NL2 did not show any processive runs within the spatial resolution limit (~250 nm) of our imaging system (Fig. 1C,D).

To test whether the charge of the neck coiled-coil domain of FRA1 affects its processivity, we generated four mutants that

targeted charged amino acids either within heptads 1 and 2 or within heptads 3 and 4 (Fig. 1B). Two of these mutants, FRA1-NCC1 and FRA1-NCC3, made the heptads more positively charged by replacing glutamic acid residues with lysine residues. Conversely, the FRA1-NCC2 and FRA1-NCC4 mutants made the heptads more negatively charged by replacing positively charged amino acids with glutamic acid. Similar to previous findings with human kinesin-1 (Thorn et al., 2000), adding positive charges to the neck coiled-coil domain increased the processivity of FRA1. FRA1-NCC1 showed ~3-fold greater processivity and moved at essentially the same speed as wild-type FRA1 (Fig. 1C,D). In contrast, FRA1-NCC3 showed an ~60% greater processivity and an ~3-fold lower speed compared to wild-type FRA1 (Fig. 1C,D). One possible

reason for why these mutations differentially affect the processivity and speed of FRA1 is that they might destabilize the neck coiled-coil to different extents, thus affecting the coordination between the two motor domains to varying degree.

Surprisingly, the FRA1-NCC2 mutant showed an ~4-fold greater processivity even though its neck coiled-coil is more negatively charged than wild-type FRA1 (Fig. 1C,D). This mutant also moved ~3-fold slower than wild-type FRA1. Why this mutant has greater processivity than FRA1-NCC1 is not clear and requires further study. In contrast to FRA1-NCC2, the FRA1-NCC4 mutant did not show processive motility under our *in vitro* conditions (Fig. 1C,D). Taken together, these results show that changing the length and

charge of the neck linker and neck coiled-coil domains modulates the processivity of FRA1 *in vitro* in a similar way to in other N-terminal kinesins (i.e. kinesins comprising their motor domains at the N-terminus).

Functional analysis of FRA1 processivity mutants *in vivo*

To determine whether the above mutations affect FRA1 processivity and function *in vivo*, we introduced them in full-length FRA1 labeled with tdTomato and stably transformed these constructs driven by the native *FRA1* promoter into the *fra1-5* knockout mutant.

Expression of wild-type FRA1-tdTomato completely rescued the dwarf phenotype of *fra1-5* plants (Fig. 2A,B). The two neck-linker
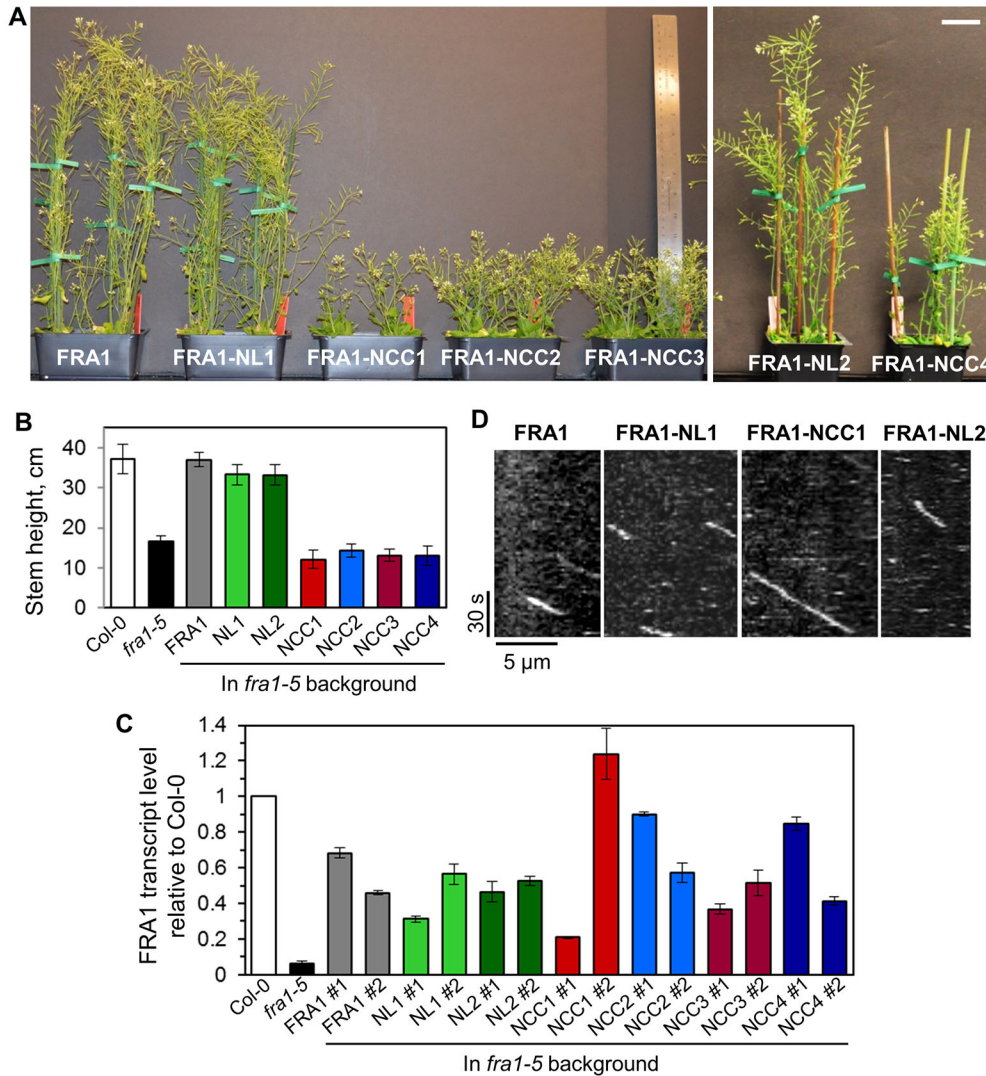
Fig. 2. *In vivo* functional and motility analysis of FRA1 neck-linker and neck coiled-coil mutants. (A) Images of 4.5-week-old *fra1-5* mutant plants expressing FRA1, FRA1-NL1, FRA1-NCC1, FRA1-NCC2, FRA1-NCC3, FRA1-NL2 or FRA1-NCC4. Scale bar: 5 cm. (B) Heights of primary inflorescence stems. Values are mean± s.d. from at least 16 plants for each genotype. (C) *FRA1* expression level relative to wild-type control. Values are mean±s.e.m. from three biological replicates. (D) Kymographs showing the movement of wild-type FRA1, FRA1-NL1, FRA1-NCC1 and FRA1-NL2 puncta at the cell cortex. (E) Motility parameters of wild-type and mutant FRA1 kinesins determined from live imaging experiments. N.A., not applicable because of extremely rare events of directional motility. Values are mean±s.d.

Protein	FRA1	FRA1-NL1	FRA1-NL2	FRA1-NCC1	FRA1-NCC2	FRA1-NCC3	FRA1-NCC4
Speed, µm/sec	0.20 ± 0.002	0.21 ± 0.004	0.13 ± 0.004	0.18 ± 0.005	N.A.	N.A.	N.A.
Run length, µm	1.27 ± 0.08	0.99 ± 0.04	1.3 ± 0.07	2.33 ± 0.08	N.A.	N.A.	N.A.
Motile density, events/µm²/min	0.025 ± 0.01	0.024 ± 0.01	0.02 ± 0.01	0.01 ± 0.01	N.A.	N.A.	N.A.
Number of molecules	121	116	117	101	16 (30 cells)	8 (28 cells)	5 (19 cells)

mutants, FRA1-NL1 and FRA1-NL2, nearly completely rescued the *fra1-5* phenotype, indicating that they are functional (Fig. 2A,B). In contrast, none of the four FRA1-NCC mutants rescued the dwarf phenotype of *fra1-5* in more than ten independent transgenic lines for each (Fig. 2A,B). This inability was not due to lack of FRA1-NCC transgene expression, as evidenced by real-time quantitative RT-PCR (qPCR) measurements of transcript abundance (Fig. 2C).

To determine whether the *in vivo* functionality of the FRA1 mutants correlates with their motility, we imaged 4-day-old hypocotyl epidermal cells using variable angle epifluorescence microscopy. Wild-type FRA1-tdTomato puncta moved an average run length of 1.3±0.08 µm at an average speed of 0.2±0.002 µm s^{-1} (mean±s.d.; Fig. 2D,E). In contrast to *in vitro* results, the run length of FRA1-NL1 puncta was ~25% lower than wild-type FRA1 at 0.99±0.04 µm while their average speed was essentially the same as wild-type FRA1. Furthermore, FRA1-NL2 was highly motile

in vivo even though it was non-motile *in vitro*. Directionally moving FRA1-NL2 puncta had a run length similar to wild-type FRA1 at 1.3±0.1 µm and an average speed of 0.13±0.01 µm s^{-1} (Fig. 2D,E). FRA1-NCC1 puncta had an ~55% greater run length than wild-type FRA1 at 2.33±0.08 µm and an average speed of 0.18±0.005 µm s^{-1}. Interestingly, even though FRA1-NCC1 is highly processive, it does not complement the *fra1-5* mutant. One potential explanation for this finding is that the motile density (i.e. the number of motile events per unit area and unit time) of FRA1-NCC1 is less than half that of wild-type FRA1 and FRA1-NL1 (Fig. 2E), which would predictably lead to less cargo transport.

The FRA1-NCC2, FRA1-NCC3 and FRA1-NCC4 mutants showed very little directional motility *in vivo* (Fig. 2E) even though FRA1-NCC2 and FRA1-NCC3 were highly processive *in vitro*. For these mutants, we frequently observed static puncta over the ~2 min imaging period, indicating that these mutants likely
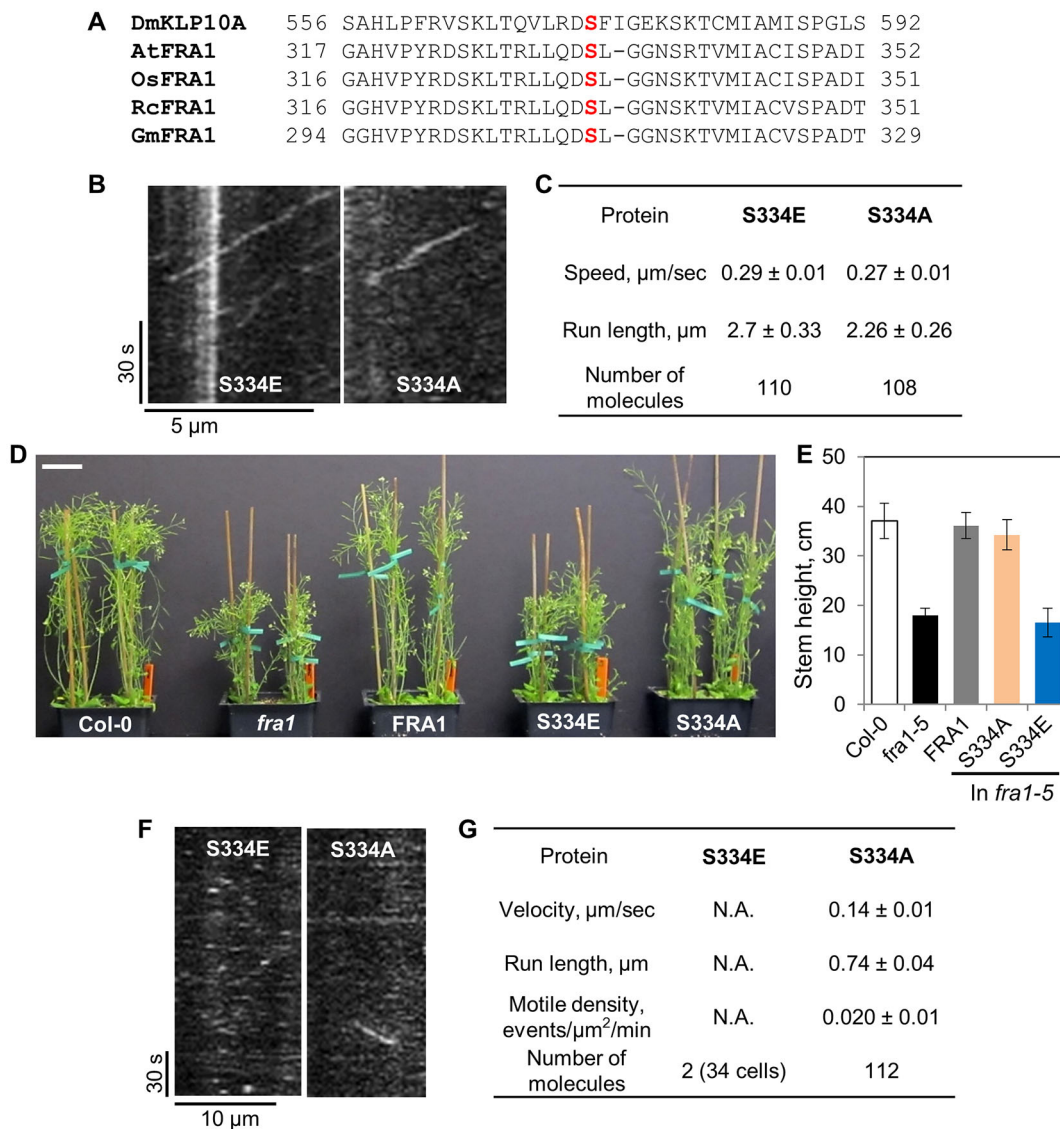
Fig. 3. Analysis of FRA1 motor domain phosphorylation mutants. (A) Sequence alignment of the α-helix 5 region of the motor domains of *Drosophila* KLP10A (DmKLP10A) and various plant FRA1 homologs. The conserved serine residue is shown in red. At, *Arabidopsis thaliana*; Os, *Oryza sativa*; Rc, *Ricinus communis*; Gm, *Glycine max*. (B) Kymographs of the FRA1 phosphorylation mutants from *in vitro* single-molecule motility assays. (C) Motility parameters of FRA1 phosphorylation mutants calculated from the *in vitro* experiments. Values are mean±s.d. (D) Images of 4.5-week-old plants. Col-0, wild-type plant. Scale bar: 5 cm. (E) Heights of primary inflorescence stems. Values are mean±s.d. from at least 16 plants for each genotype. (F) Kymographs showing the movement of FRA1-S334A and FRA1-S334E puncta at the cell cortex. (G) Motility parameters of FRA1-S334A and FRA1-S334E determined from live imaging experiments. N.A., not applicable because of extremely rare events of directional motility. Values are mean±s.d.

bind to microtubules *in vivo* but lack processive motility. Based on these data, we conclude that a high level of processive motility is necessary for the function of FRA1 in plants.

Mutation of a conserved serine residue in the FRA1 motor domain alters its motility

Phosphorylation of a conserved serine residue in the motor domain of the *Drosophila melanogaster* kinesin-13 KLP10A has been shown to decrease its microtubule-depolymerizing activity without altering its microtubule binding (Mennella et al., 2009). Sequence alignment with the motor domains of plant FRA1 homologs showed that this serine residue is conserved within the microtubule binding α-helix 5 of these kinesins (Fig. 3A). To determine whether this serine potentially plays a role in regulating FRA1 motility, we generated phosphomimetic (FRA1-S334E) and nonphosphorylatable (FRA1-S334A) versions of both FRA1(707)–GFP and full-length FRA1-tdTomato.

In vitro, FRA1-S334E and FRA1-S334A showed ∼33% and ∼22% increased processivity and ∼18% and ∼23% decreased speed compared to wild-type FRA1, respectively (Fig. 3B,C). However, we found that FRA1-S334A was able to rescue the dwarf *fra1-5* phenotype, whereas FRA1-S334E was not (Fig. 3D,E). Live imaging showed that genetic complementation correlated with the motility of these mutant kinesins. Specifically, the FRA1-S334A mutant was motile whereas the FRA1-S334E mutant was non-motile (Fig. 3F,G). Notably, FRA1-S334A is functional even though its average run length and speed *in vivo* are ∼40% and ∼25% less than that of wild-type FRA1, respectively (Fig. 3G). However, the motile density of FRA1-S334A is similar to that of wild-type FRA1 (Fig. 3G), indicating that lower kinesin processivity and speed are tolerated as long as sufficient numbers of molecules are engaged in transport.

Overexpression of FRA1 phenocopies the *fra1-5* mutant due to gene silencing

Overexpression of FRA1 has been found to phenocopy *fra1* loss-of-function mutants (Zhou et al., 2007); however, the underlying

mechanism remains unknown. An increase in kinesin density can decrease processivity *in vitro* by overcrowding the microtubule lattice (Leduc et al., 2012; Telley et al., 2009). Therefore, one possible mechanism for the FRA1 overexpression phenotype is that it creates traffic jams along cortical microtubules, thus reducing processivity and compromising FRA1 function. To test this hypothesis, we expressed wild-type FRA1–tdTomato driven by a constitutive 35S promoter in wild-type *Arabidopsis* plants. Similar to previous work, our FRA1-overexpression lines mimicked the dwarf stem phenotype of *fra1-5* plants (Fig. 4A,B). However, transcript analysis by using qPCR revealed that *FRA1* expression was greatly reduced in these plants (Fig. 4C). In addition, immunoblot analysis showed that endogenous FRA1 protein was undetectable in these plants (Fig. 4D). Using live imaging, we also found that FRA1–tdTomato was essentially undetectable at the cell cortex in these plants. Therefore, both endogenous and transgenic *FRA1* expression were suppressed, probably due to 35S-promoter-triggered gene silencing (Daxinger et al., 2008; Mishiba et al., 2005; Mlotshwa et al., 2010). These findings explain why FRA1 'overexpression' lines show remarkably similar developmental and cell wall phenotypes to those in the knockout *fra1-5* line (Zhou et al., 2007).

Summary

Our data show that abundant and processive motility are important for the function of FRA1 *in vivo*, consistent with a proposed vesicular trafficking function of FRA1. While several studies have analyzed kinesin processivity mutants *in vitro*, to the best of our knowledge, this is the first study to measure the motility of these mutants *in vivo*. There are several possibilities as to why there are significant differences between the *in vitro* and *in vivo* behavior of the various FRA1 mutants. It is known that kinesin mutants with positively charged residues introduced in the NL and NCC domains show greater processivity *in vitro* due to electrostatic interactions with the negatively charged C-terminus of tubulin under low ionic strength conditions (Shastry and Hancock, 2010; Thorn et al., 2000). In cells,
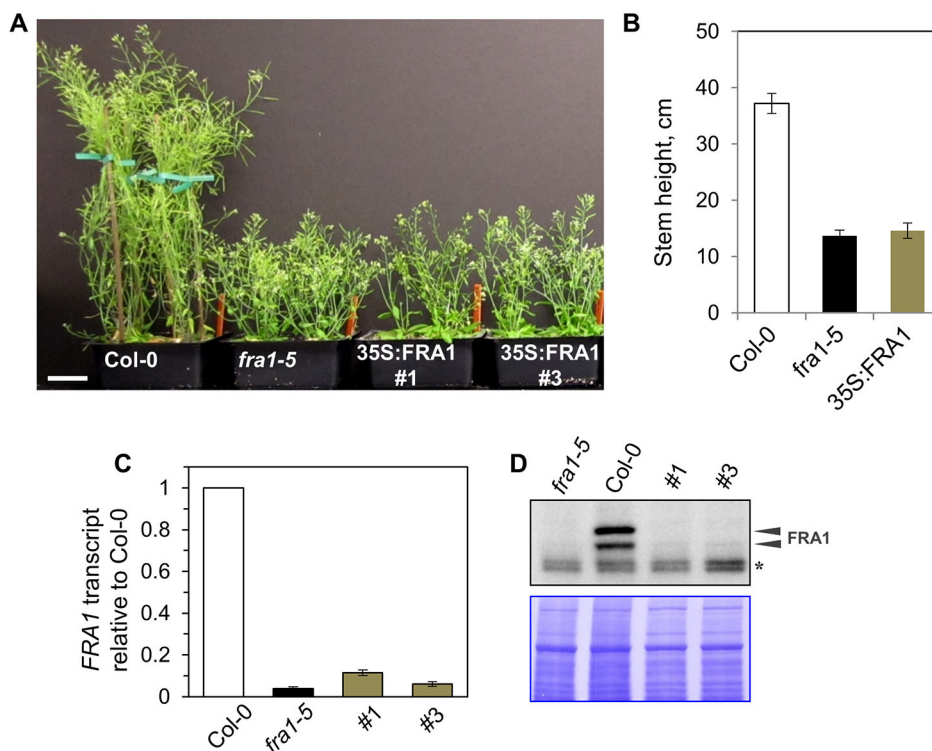
Fig. 4. Effect of *FRA1* overexpression in wild-type plants. (A) Images of 4.5-week-old plants. Col-0, wild-type plant; 35S:FRA1, plants expressing 35S-promoter-driven FRA1–tdTomato. Scale bar: 5 cm. (B) Heights of primary inflorescence stems. Values are mean±s.d. from at least eight plants for each genotype. (C) *FRA1* expression level relative to wild-type control. Values are mean±s.e.m. from three biological replicates. (D) Immunoblot of the native FRA1 protein in *fra1-5*, Col-0 and two independent transformants expressing 35S-driven FRA1–tdTomato. The native FRA1 protein shows up as two bands (arrowheads). The asterisk marks a non-specific band.

the higher cytoplasmic ionic strength likely disrupts these electrostatic effects, thus reducing the gain in processivity. Furthermore, the *in vitro* motility assays are conducted using a truncated kinesin lacking the tail domain and in the absence of cargo and external load. Interactions between the motor and tail domains are critical for regulating kinesin motility (Hammond et al., 2009; Hirokawa et al., 1989), which might account for altered motility of full-length kinesin *in vivo*. Moreover, full-length kinesin transporting cargo in cells will experience load, which can promote kinesin stalling and detachment from microtubules (Svoboda and Block, 1994; Valentine and Block, 2009), thus impacting processivity. In addition, regulatory proteins can alter kinesin motility in cells compared to *in vitro* conditions. Therefore, while *in vitro* experiments are helpful to identify potential mechanisms underlying kinesin mechanochemistry, they must be tested *in vivo* to verify their operation under physiological conditions.

MATERIALS AND METHODS

Plant materials and growth

Seeds were sterilized with 25% bleach for 10 min, washed with sterile water three times and plated on 0.5× Murashige and Skoog medium (Caisson Laboratories). For live imaging, seeds were stratified for 2–3 days at 4°C and then grown under 16 h light for 4 days. For phenotypic analysis, plants were grown in soil under continuous light at 22°C.

Construct preparation

The FRA1(707)–GFP and proFRA1::FRA1-tdTomato constructs (AT5G47820) have been previously described in Zhu and Dixit (2011) and Zhu et al. (2015), respectively. For the 35S::FRA1-tdTomato construct, the FRA1–tdTomato insert was ligated using HindIII and Sal1 restriction sites downstream of the 35S CaMV promoter in pCAMBIA1300. For the processivity mutants, site-directed mutagenesis was conducted using the megaprimers listed in Table S1.

qPCR and immunoblotting

RNA and proteins were isolated from 2-week-old seedlings. Total RNA was extracted by the TRIzol method and complementary DNA (cDNA) synthesized with revertAid First Strand cDNA Synthesis Kit (ThermoFisher Scientific). qPCR was performed using the SYBR method with primers listed in Zhu et al. (2015).

For immunoblotting, lysates were prepared by grinding seedlings in liquid N_2 and homogenizing in protein isolation buffer (50 mM Tris-acetate, pH 7.5, 2 mM EDTA, 1 mM PMSF and protease inhibitor tablet from Roche). Total proteins (∼30 µg each) were separated by SDS-PAGE, transferred onto PVDF membrane and probed with anti-FRA1 primary antibody (1:1000; Zhu et al., 2015) and horseradish peroxidase (HRP)-conjugated anti-rabbit IgG secondary antibody (1:5000, Jackson ImmunoResearch).

Protein purification and *in vitro* motility assays

His-tagged FRA1(707)–GFP was expressed in BL21(DE3) Rosetta *Escherichia coli* using 0.5 mM IPTG at 24°C for 4 h and purified using Ni–NTA resin affinity chromatography (Qiagen). The purified fusion protein was then desalted using a PD-10 column (Amersham Biosciences) and exchanged into MAB buffer (10 mM PIPES, 50 mM potassium acetate, 4 mM $MgSO_4$, 1 mM EGTA, pH 7.0) supplemented with 50 mM NaCl, which has an ionic strength of ∼110 mM. Single-molecule motility assays were carried out exactly as described in Zhu and Dixit (2011).

Live imaging and data analysis

Live imaging of FRA1–tdTomato was carried out in apical hypocotyl cells of 4-day-old seedlings using variable angle epifluorescence microscopy. Specimens were excited with 3 mW 561-nm laser (Melles Griot) and images gathered using a 100× (NA 1.45) objective at 1-s intervals with an EM-CCD camera (ImagEM, Hamamatsu). Kymograph analysis was used to measure the speed and run length for individual motile events. The mean speed was

determined by Gaussian fitting using the least-squares method to the measured speed distribution. For the mean run length, cumulative distribution functions (CDFs) were calculated from the distributions of measured run lengths and a monoexponential function was fitted to 1-CDF data using the least-squares method.

References

Bringmann, H., Skiniotis, G., Spilker, A., Kandels-Lewis, S., Vernos, I. and Surrey, T. (2004). A kinesin-like motor inhibits microtubule dynamic instability. *Science* **303**, 1519-1522.

Daxinger, L., Hunter, B., Sheikh, M., Jauvion, V., Gasciolli, V., Vaucheret, H., Matzke, M. and Furner, I. (2008). Unexpected silencing effects from T-DNA tags in Arabidopsis. *Trends Plant Sci.* **13**, 4-6.

Desai, A., Verma, S., Mitchison, T. J. and Walczak, C. E. (1999). Kin I kinesins are microtubule-destabilizing enzymes. *Cell* **96**, 69-78.

Gupta, M. L., Jr, Carvalho, P., Roof, D. M. and Pellman, D. (2006). Plus end-specific depolymerase activity of Kip3, a kinesin-8 protein, explains its role in positioning the yeast mitotic spindle. *Nat. Cell Biol.* **8**, 913-923.

Hall, D. H. and Hedgecock, E. M. (1991). Kinesin-related gene unc-104 is required for axonal transport of synaptic vesicles in C. elegans. *Cell* **65**, 837-847.

Hammond, J. W., Cai, D. W., Blasius, T. L., Li, Z., Jiang, Y. Y., Jih, G. T., Meyhofer, E. and Verhey, K. J. (2009). Mammalian kinesin-3 motors are dimeric in vivo and move by processive motility upon release of autoinhibition. *PLoS Biol.* **7**, 650-663.

Hirokawa, N., Pfister, K. K., Yorifuji, H., Wagner, M. C., Brady, S. T. and Bloom, G. S. (1989). Submolecular domains of bovine brain kinesin identified by electron microscopy and monoclonal antibody decoration. *Cell* **56**, 867-878.

Howard, J., Hudspeth, A. J. and Vale, R. D. (1989). Movement of microtubules by single kinesin molecules. *Nature* **342**, 154-158.

Kanai, Y., Okada, Y., Tanaka, Y., Harada, A., Terada, S. and Hirokawa, N. (2000). KIF5C, a novel neuronal kinesin enriched in motor neurons. *J. Neurosci.* **20**, 6374-6384.

Kondo, S., Sato-Yoshitake, R., Noda, Y., Aizawa, H., Nakata, T., Matsuura, Y. and Hirokawa, N. (1994). KIF3A is a new microtubule-based anterograde motor in the nerve axon. *J. Cell Biol.* **125**, 1095-1107.

Kong, Z., Ioki, M., Braybrook, S., Li, S., Ye, Z.-H., Lee, Y.-R. J., Hotta, T., Chang, A., Tian, J., Wang, G. et al. (2015). Kinesin-4 functions in vesicular transport on cortical microtubules and regulates cell wall mechanics during cell elongation in plants. *Mol. Plant* **8**, 1011-1023.

Kurasawa, Y., Earnshaw, W. C., Mochizuki, Y., Dohmae, N. and Todokoro, K. (2004). Essential roles of KIF4 and its binding partner PRC1 in organized central spindle midzone formation. *EMBO J.* **23**, 3237-3248.

Leduc, C., Padberg-Gehle, K., Varga, V., Helbing, D., Diez, S. and Howard, J. (2012). Molecular crowding creates traffic jams of kinesin motors on microtubules. *Proc. Natl. Acad. Sci. USA* **109**, 6100-6105.

Mennella, V., Tan, D.-Y., Buster, D. W., Asenjo, A. B., Rath, U., Ma, A., Sosa, H. J. and Sharp, D. J. (2009). Motor domain phosphorylation and regulation of the Drosophila kinesin 13, KLP10A. *J. Cell Biol.* **186**, 481-490.

Mishiba, K., Nishihara, M., Nakatsuka, T., Abe, Y., Hirano, H., Yokoi, T., Kikuchi, A. and Yamamura, S. (2005). Consistent transcriptional silencing of 35S-driven transgenes in gentian. *Plant J.* **44**, 541-556.

Mlotshwa, S., Pruss, G. J., Gao, Z., Mgutshini, N. L., Li, J., Chen, X., Bowman, L. H. and Vance, V. (2010). Transcriptional silencing induced by Arabidopsis T-DNA mutants is associated with 35S promoter siRNAs and requires genes involved in siRNA-mediated chromatin silencing. *Plant J.* **64**, 699-704.

Okada, Y., Yamazaki, H., Sekine-Aizawa, Y. and Hirokawa, N. (1995). The neuron-specific kinesin superfamily protein KIF1A is a unique monomeric motor for anterograde axonal transport of synaptic vesicle precursors. *Cell* **81**, 769-780.

Richardson, D. N., Simmons, M. P. and Reddy, A. S. N. (2006). Comprehensive comparative analysis of kinesins in photosynthetic eukaryotes. *BMC Genomics* **7**, 18.

Shastry, S. and Hancock, W. O. (2010). Neck linker length determines the degree of processivity in kinesin-1 and kinesin-2 motors. *Curr. Biol.* **20**, 939-943.

Shastry, S. and Hancock, W. O. (2011). Interhead tension determines processivity across diverse N-terminal kinesins. *Proc. Natl. Acad. Sci. USA* **108**, 16253-16258.

Soppina, V., Norris, S. R., Dizaji, A. S., Kortus, M., Veatch, S., Peckham, M. and Verhey, K. J. (2014). Dimerization of mammalian kinesin-3 motors results in superprocessive motion. *Proc. Natl. Acad. Sci. USA* **111**, 5562-5567.

Svoboda, K. and Block, S. M. (1994). Force and velocity measured for single kinesin molecules. *Cell* **77**, 773-784.

Telley, I. A., Bieling, P. and Surrey, T. (2009). Obstacles on the microtubule reduce the processivity of Kinesin-1 in a minimal in vitro system and in cell extract. *Biophys. J.* **96**, 3341-3353.

Thorn, K. S., Ubersax, J. A. and Vale, R. D. (2000). Engineering the processive run length of the kinesin motor. *J. Cell Biol.* **151**, 1093-1100.

Vale, R. D., Reese, T. S. and Sheetz, M. P. (1985). Identification of a novel force-generating protein, kinesin, involved in microtubule-based motility. *Cell* **42**, 39-50.

Valentine, M. T. and Block, S. M. (2009). Force and premature binding of ADP can regulate the processivity of individual Eg5 dimers. *Biophys. J.* **97**, 1671-1677.

Varga, V., Helenius, J., Tanaka, K., Hyman, A. A., Tanaka, T. U. and Howard, J. (2006). Yeast kinesin-8 depolymerizes microtubules in a length-dependent manner. *Nat. Cell Biol.* **8**, 957-962.

Verhey, K. J., Meyer, D., Deehan, R., Blenis, J., Schnapp, B. J., Rapoport, T. A. and Margolis, B. (2001). Cargo of kinesin identified as JIP scaffolding proteins and associated signaling molecules. *J. Cell Biol.* **152**, 959-970.

Walczak, C. E., Mitchison, T. J. and Desai, A. (1996). XKCM1: a Xenopus kinesin-related protein that regulates microtubule dynamics during mitotic spindle assembly. *Cell* **84**, 37-47.

Yamazaki, H., Nakata, T., Okada, Y. and Hirokawa, N. (1995). KIF3A/B: a heterodimeric kinesin superfamily protein that works as a microtubule plus end-directed motor for membrane organelle transport. *J. Cell Biol.* **130**, 1387-1399.

Zhou, J., Qiu, J. and Ye, Z.-H. (2007). Alteration in secondary wall deposition by overexpression of the Fragile Fiber 1 kinesin-like protein in Arabidopsis. *J. Int. Plant Biol.* **49**, 1235-1243.

Zhu, C. and Dixit, R. (2011). Single molecule analysis of the Arabidopsis FRA1 kinesin shows that it is a functional motor protein with unusually high processivity. *Mol. Plant* **4**, 879-885.

Zhu, C. and Dixit, R. (2012). Functions of the Arabidopsis kinesin superfamily of microtubule-based motor proteins. *Protoplasma* **249**, 887-899.

Zhu, C., Ganguly, A., Baskin, T. I., McClosky, D. D., Anderson, C. T., Foster, C., Meunier, K. A., Okamoto, R., Berg, H. and Dixit, R. (2015). The fragile Fiber1 kinesin contributes to cortical microtubule-mediated trafficking of cell wall components. *Plant Physiol.* **167**, 780-792.

Supplemental Table 1: Primers used in this study

Mutation	Primer sequence
FRA1-NL1	CCTGTTGTTAATAGAGATGCTAAGTCTAGTGAGATGC
FRA1-NL2	CCTGTTGTTAATAGAGATCCTGTGGATGCTCTGTCTAGTGAGATGC
FRA1-NCC1	CCTGTGTCTAGTAAGATGCTAAAAATGAAGCAACAGAAGAAGTACTTGCAGGCAAAACTCTCC
FRA1-NCC2	GAGATGCTAGAAATGGAACAACAGGAAGAATACTTGCAGGCAGAACTCTCCTTAGAGACCGGAGGA
FRA1-NCC3	CCTCATGTGCAAAAGTACAGGCTCTTAAAAAAAGGATTGTTTGGCTTAAAACTGCTAATAAGAAACTTTGCCGCGAAC
FRA1-NCC4	GTACAGGCTCTTGAAGAAGAGATTGTTTGGCTTGAAACTGCTGAAGAAGAACTTTGCGAGGAACTTCATGAG
FRA1-S334A	GCTGTTACCACCAAGGGCATCCTGCAAAAGCCG
FRA1-S334E	GCTGTACCACCAAGTTCATCCTGCAAAAGCCG